

RESEARCH PAPER

EXPERIMENTAL DETERMINATION OF THE DRAW BEAD COEFFICIENT OF FRICTION OF CuZn SHEETS IN SHEET METAL FORMING PROCESSES

Tomasz Trzepieciński¹, Valmir Dias Luiz², Marcin Szpunar³

¹ Department of Manufacturing Processes and Production Engineering, Faculty of Mechanical Engineering and Aeronautics, Rzeszow University of Technology, al. Powstancow Warszawy 8, 35-959 Rzeszów, Poland

² Department of Metallurgy and Chemistry, Centro Federal de Educação Tecnológica de Minas Gerais, R. 19 de Novembro, 121, Centro Norte, Timóteo, MG, 35180-008, Brazil

³ Doctoral School of Engineering and Technical Sciences at the Rzeszow University of Technology, al. Powstancow Warszawy 12, 35-959 Rzeszów, Poland

*Corresponding author: tomtr@prz.edu.pl, tel.: +48178651574, Faculty of Mechanical Engineering and Aeronautics, Rzeszow University of Technology, al. Powstancow Warszawy 8, 35-959 Rzeszów, Poland

Received: 11.04.2023

Accepted: 13.07.2023

ABSTRACT

In sheet metal forming, draw beads are used to limit the flow of sheet metal in specific areas of the stamping die. The value of the coefficient of friction at the draw bead determines the achievement of the desired resistance to sheet displacement. This article presents the results of experimental tests for determining the coefficient of friction on a draw bead using a specially developed tribotester. The test material consisted of CuZn37, CuZn30 and CuZn10 brass sheets in various states of hardening. Investigations were carried out with different roughness of the counter samples and sliding speeds. In addition, the tests were carried out under conditions of dry friction and lubrication of the sheet surface with LAN-46 machine oil. The relationships between the process parameters and the value of the coefficient of friction were analysed using the analysis of variance. It was found that the coefficient of friction decreases with increasing mean roughness of the counter samples. Lubrication reduced friction by about 6.2-29.8% depending on the grade of the tested sheet and the sliding speed.

Keywords: analysis of variance; brass sheets; coefficient of friction; draw bead; sheet metal forming

INTRODUCTION

Among the factors influencing tribological phenomena in plastic forming processes, the following should be mentioned: geometry of contact, kinematics of tool movement, load dynamics, physicochemical phenomena on the contact surface and temperature [1, 2]. Friction forces occurring on the contact surface of metals have a significant impact on the course of the sheet metal forming process [3, 4]. Due to the occurrence of different conditions in particular areas of the drawpiece in terms of the state of strain and stress, a number of tests modelling the friction conditions in selected areas of the drawpiece have been developed [5, 6]:

- strip drawing test,
- strip tension test,
- bending under tension test,
- draw bead test,
- pin-on-disc tribometers.

Friction reduces the surface quality of the drawpieces and increases tool wear. The most effective method of reducing the friction value is to lubricate the sheet metal surface [7]. There are very many different types of lubricants in use for sheet metal forming (SMF) operations. The following lubricants are used in SMF: oily emulsions, non-emulsifiable oils as well as consistent

lubricants such as pastes, greases, soaps, waxes, and solid lubricants [8]. Emulsifiable oil concentrates can be diluted with water to achieve desired viscosity. Depending on the concentrations two grades of emulsions are formed: water-in-oil and oil-in-water. Water provides a cooling effect during the SMF. Non-emulsifiable oils differ in the presence and concentration of lubricity antiwear (AW) and extreme pressure (EP) additives and nonpolar and polar additives. Solid lubricants, pastes, waxes, greases and tixotropic oils are obtained when insoluble thickeners like solid paraffins, pigments or soaps are added to the oily emulsions and straight oils.

Lubricating greases are colloidal systems in which a thickener is dispersed in a carrier liquid. The thickener creates a flexible, spatial network structure that binds the liquid phase, giving the grease the required consistency. The liquid component can be mineral oil or synthetic lubricant [9]. In addition to salts, complex soaps, which are salts of fatty acids and low molecular weight organic acids, are used as thickeners [9].

Mineral oils are complex mixtures of high-boiling saturated and aromatic hydrocarbons containing from 20 to 40 carbon atoms in a molecule [10]. Mineral oils obtained in the process of vacuum distillation contain mainly isoparaffinic and 1-3-ring naphthenic hydrocarbons with long-chain alkyl substituents, 2-3-ring naphthenic-aromatic and aromatic hydrocarbons, including mainly alkylbenzenes with long alkyl chains. Synthetic oils are

chemically homogeneous organic compounds obtained by syntheses. They can be divided into hydrocarbon and ester oils, including esters of organic, phosphoric and carbonic acids, polyalkyl glycol oils and their esters [10].

In sheet metal forming, many types of lubricants are used, adapted to the prevailing values, process temperature and the specificity of the machining process [11, 12].

Determining the influence of the friction process parameters on the value of the coefficient of friction is difficult due to the complexity of the relationship between the individual parameters [13,14]. Many parameters are correlated with each other, causing a synergistic effect [1]. As qualitative analysis of the friction process is difficult, analytical tools are used, such as analysis of variance, artificial neural networks, machine learning methods, genetic algorithms and the Taguchi method. Dilmeç and Arap [15] studied the effects of the surface roughness of the tools, the drawing speed, and lubrication on the friction coefficient using the analysis of variance (ANOVA). It was found that the coefficient of friction was significantly different in specific areas of the drawpiece. Dechjarerna and Kamonrattanapisu [16] investigated the influence of the draw bead parameters (draw bead height and shoulder radius) on the thinning distributions of the drawpieces. The ANOVA results show that the shoulder radius is the most important parameter influencing the thinning distribution. Ma et al. [17] studied the significant factors affecting the tribological behaviour of commercial pure titanium sheets in warm forming. Their results revealed that the friction and lubrication conditions are not constant and are greatly dependent on the process parameters. Carvalho and Lukács [18] used ANOVA to study the role of friction in the strip drawing test. The lower velocity has resulted in an increasing coefficient of friction. In this article, the analysis of variance was used to determine the relationships between the parameters of the friction process and the value of the coefficient of friction. The value of the coefficient of friction of brass sheets was determined based on the experimental results of the draw bead test. Friction tests were carried out under different friction conditions, for different counterexample roughness and at different sliding speeds.

MATERIAL AND METHODS

Test material

Three grades of brass sheets 0.7-mm-thick CuZn37 z6, 0.4-mm-thick CuZn30 z4 and 1-mm-thick CuZn10 z4 were tested. The samples for the friction test were strips approximately 200 mm long and 20 mm wide (Fig. 1). The mechanical properties of the sheets (Table 1) were determined by tensile testing using a uniaxial testing machine. The values of the roughness parameters (Table 2) were determined using the Surtronic 3+ measuring system by Taylor Hobson.

Table 1 Basic mechanical parameters of the test materials

Material	Yield stress, MPa	Ultimate tensile stress, MPa	Elongation A50
CuZn10 z4	346	384	0.12
CuZn30 z4	120	280	0.05
CuZn37 z6	474	516	0.07

Table 2 Basic surface roughness parameters of the test materials

Material	Ra, µm	Rt, µm	Rq, µm
CuZn10 z4	0.41	6.1	0.58
CuZn30 z4	0.14	1.4	0.18
CuZn37 z6	0.14	2.9	0.26



Fig. 1 Photograph of the strip sample

Experimental procedures

Friction tests were carried out using a specially designed tester (Fig. 2). The idea of the draw bead test is the ability to separate sheet plastic deformation resistance from frictional resistance. Therefore, the test consists of two stages:

- pulling the sheet metal with fixed counter samples,
- pulling the sheet metal with freely rotating counter samples.

The pulling force and clamping force are measured in both tests (Fig. 3). The difference in the pulling force for the system of freely rotating and fixed rollers can be attributed to the friction process and used to calculate the value of the coefficient of friction according to the relationship [19]:

$$\mu = \frac{1}{\pi} \frac{F_P - F_R}{F_C} \tag{1.}$$

where F_P is the pulling force with the fixed counter samples, F_R is the pulling force with the freely rotating counter samples, and F_C is the clamping force obtained with fixed draw beads.



Fig. 2 Photograph of the friction tester

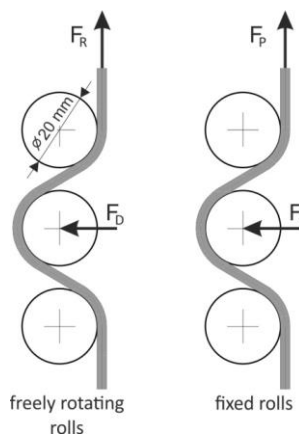


Fig. 3 The forces in the draw bead tests

Counterexamples (rolls) with a diameter of 20 mm and a width of 22 mm were made of cold-work tool steel. Four sets of rolls

with average roughness Ra equal to 2.5, 1.25, 0.63 and 0.32 μm , were tested. Two sliding speeds (0.05 and 0.15 m/min) were considered. The tests were carried out under conditions of dry friction and lubrication with LAN-46 machine oil (kinematic viscosity at 40°C, $\eta = 43.9 \text{ mm}^2/\text{s}$). The lubricant was distributed uniformly on the surface of the samples using a shaft. The tests were conducted at room temperature.

Analysis of variance

To determine the influence of the input factors on the coefficient of friction (COF) output, the analysis of variance has been investigated. The sliding speed (coded A) and Ra parameter of counter samples (coded B) have been defined as numeric input factors while the sheet material (coded C) and contact type (coded D) are categorical input factors. Coefficient of friction was set as response of ANOVA model.

RESULTS AND DISCUSSION

A tendency for the coefficient of friction to decrease was observed with increasing mean roughness of the counter samples (Fig. 4). The greater mean roughness of the counter samples means a decrease in the real contact area and, consequently, the metallic contact between the cooperating surfaces is limited. On the other hand, larger spaces between the surface asperities of the cooperating surfaces can accommodate more lubricant. It should also be noted that the surface roughness of the sheet in the draw bead test is constantly evolving due to the repeated bending and straightening of the sheet as the sample passes through the draw bead. In addition, the properties of the sheet change as a result of the work-hardening phenomenon. These properties change as the sheet passes through successive counter samples. So, the value of the coefficient of friction determined by Eq. 1 should be considered as an average value, which was previously noted by Nine [19]. The CuZn30 z6 and CuZn37 z6 sheets were characterised by the same average roughness Ra = 0.14 mm, so the differences in the value of the coefficient of friction of these sheets can be attributed to different mechanical properties. The yield strength of the CuZn30 z6 sheet (120 MPa) is more than three times higher than that of the CuZn37 z6 sheet (474 MPa). As shown [20] that the friction behaviour of metals is that harder metals exhibit lower COFs than softer metals. This microscopic change of the flattened area due to plastic deformation was observed in the case of materials without work hardening [21]. The degree of surface roughening for materials without work hardening is more intense [22].

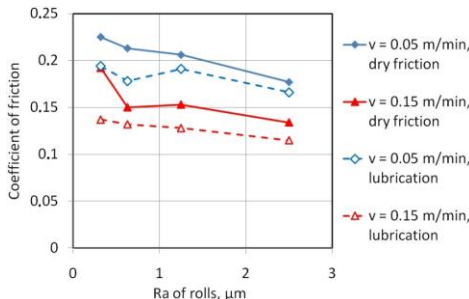


Fig. 4 The effect of the friction conditions on the coefficient of friction for CuZn37 z6 material

The sliding speed affects the reduction of the coefficient of friction under conditions of both dry friction and machine oil lubrication. At a sliding speed of 0.05 m/min, the use of lubricant

reduces the coefficient of friction of the CuZn37 z6, CuZn30 z4 and CuZn10 z4 sheets by about 6.2–16.4% (Fig. 4), 19.4–24.6% (Fig. 5) and 16.3–23.2% (Fig. 6), respectively. At a sliding speed of 0.15 m/min, the use of grease reduces the coefficient of friction of the CuZn37 z6, CuZn30 z4 and CuZn10 z4 sheets by about 12.0–28.6% (Fig. 2), 15.3–21.3% (Fig. 5) and 17.0–29.8% (Fig. 6), respectively.

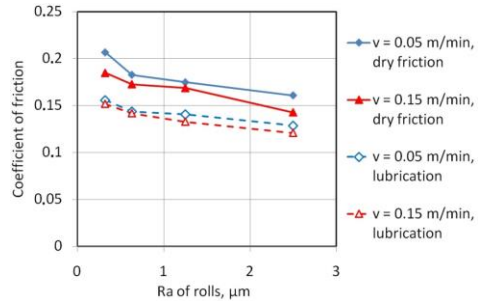


Fig. 5 The effect of the friction conditions on the coefficient of friction for CuZn30 z4 material

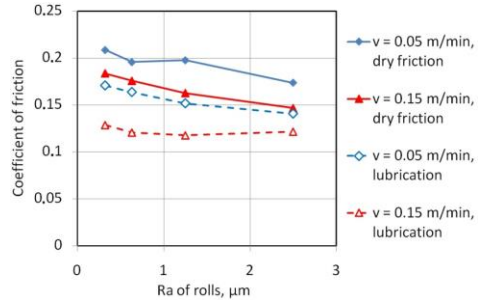


Fig. 6 The effect of the friction conditions on the coefficient of friction for CuZn10 z4 material

Attention should be paid to the difference between the phenomenon of friction occurring in the kinematic nodes of machines (i.e. bearings) and in the processes of sheet metal forming. In machine nodes, it is possible to optimise friction and wear by improving the properties of the cooperating materials [23,24]. In sheet metal forming, there is contact between sheet metal of much lower strength and a tool of much higher strength and hardness. Hence, the optimisation of the friction conditions in sheet metal forming is possible only by changing the properties of the tool and the lubricants used [25].

The ANOVA for different degrees of regression models shows that the two-factor interaction (2FI) model is the most beneficial while the quadratic model seems to be aliased. As selection criteria, sequential p-values lower than 0.05 along with highest Adjusted R² and Predicted R² have been determined (Table 3).

Table 3 Model selection criteria – fit summary

Source	Sequential p-value	Adjusted R ²	Predicted R ²	Decision
Linear	< 0.0001	0.8192	0.7901	Rejected
2FI	< 0.0001	0.9362	0.9075	Selected
Quadratic	0.1013	0.9399	0.9119	Aliased

Finally, the 2FI model was chosen, however in the next step a backward elimination algorithm has been applied. This algorithm reduces model sources which are not significant (p-value

less than 0.05) starting with the highest model degrees, resulting in the exclusion of AD, AB and BC. The ANOVA for the reduced 2FI model is shown in Tables 4 and 5.

Table 4 ANOVA with fit statistics for the reduced two-factor interactions model

Source	Sum of squares	df	Mean square	F-value	p-value
Model	0.0371	10	0.0037	73.89	< 0.0001
A – sliding speed	0.0112	1	0.0112	222.55	< 0.0001
B – Ra of counter-samples	0.0066	1	0.0066	130.74	< 0.0001
C – sheet material	0.0010	2	0.0005	10.34	0.0003
D – contact type	0.0139	1	0.0139	276.55	< 0.0001
AC	0.0034	2	0.0017	34.13	< 0.0001
BD	0.0006	1	0.0006	11.03	0.0020
CD	0.0005	2	0.0002	4.52	0.0175
Residual	0.0019	37	0.0001		
Total correlation	0.0389	47			

Table 5 Fit statistics of the ANOVA model

Standard deviation	0.0071	R ²	0.9523
mean	0.1619	adjusted R ²	0.9394
C.V., %	4.38	predicted R ²	0.9201
		adequacy precision	37.7329

The F-value of the model is 73.89, indicating the model is significant. There is only 0.01% of probability that this big F-value will occur due to noise. The Predicted R² of 0.9201 and the Adjusted R² of 0.9394 is reasonable, meaning that the difference is less than 0.2 (Table 6). Adequacy precision measures the signal-to-noise ratio. More than four is desirable. The 32.7329 ratio indicates sufficient signals and means the model can be used to navigate the design space.

In the next step, diagnostic analysis has been carried out for the obtained model. Figure 7 presents Cook's distance in terms of the subsequent runs. The plot shows how much the regression will change if the case is deleted. Relatively large values are associated with high leverage and large student residuals. Large values should be examined – they may be caused by errors in recording, inaccurate models or design points that are far from other cases. The red line is the limit for the low values which is set as the critical F-value at an alpha of 0.5 using p and n-p degrees of freedom, where p means the number of terms in the model including the intercept and n is the number of runs.

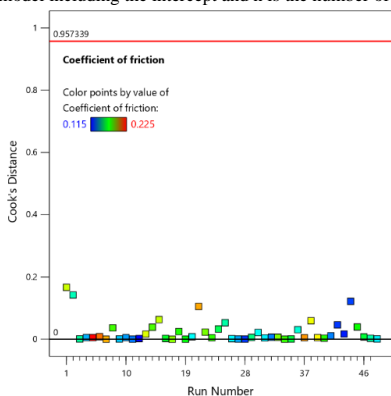


Fig. 7 Diagnostics plots for the ANOVA model: Cook's distance

Figure 8 shows the predicted values for the created model compared to the actual measured ones. The data points should be deployed close to the 45 degree line.

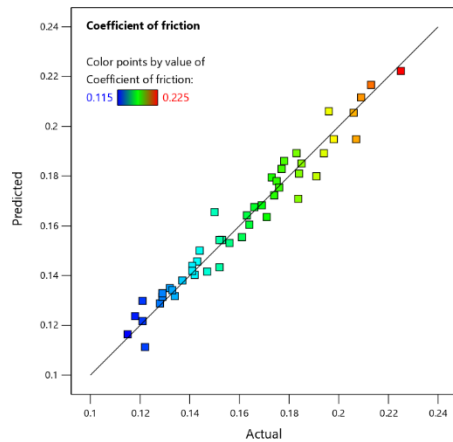


Fig. 8 Diagnostics plots for the ANOVA model: Predicted vs. actual COF values

The plot presented in Figure 9 is the externally studentized residuals versus the experimental run order.

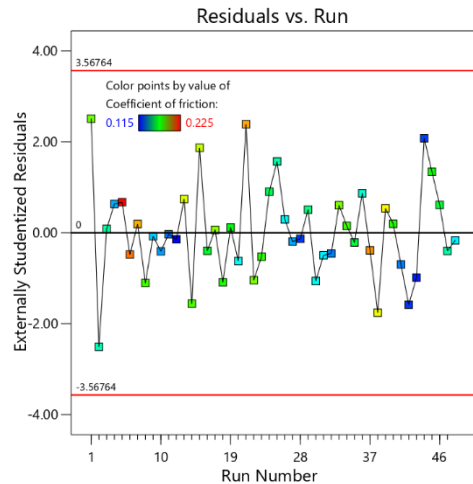


Fig. 9 Diagnostics plots for the ANOVA model: externally studentized residuals vs. run number

This check helps detect hidden variables that may affect the response during the experiment. This plot should be a random distribution, and the time-related trend indicates that some variable is lurking in the background and affecting the experiment. The externally studentized residual referred to as outlier-t controls whether a run is consistent with the other runs, assuming the chosen model holds. The model coefficient is calculated on the basis of all design points except one. The response at that time will be predicted. The residuals are evaluated using the t-test. If the value exceeds the calculated limit it should be considered a possible outlier. The difference in the fits plot (DFFITs) measures the influence of the *i*th observation on the predicted

value. It is determined by observing the change in predicted values that occurs when that response value is absent. Low values are required. The higher the value of the DFFITS, the greater it influences the fitted model. A different way to define the DFFITS is it is the externally studentized residuals enlarged at high leverage points and decreased at low leverage points. A run is found to be influential when the DFFITS value is outside the calculated limits. The calculated DFFITS values are within the limits (Fig. 10).

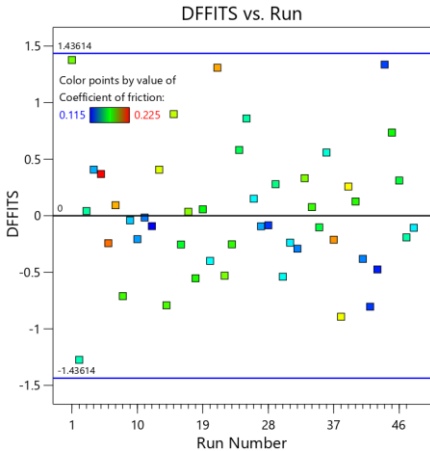


Fig. 10 Diagnostics plots for the ANOVA model: DFFITS vs. run number

By analyzing the contour plots, a tendency for the COF to reduce can be found with an increasing Ra parameter of the counter samples as well as the sliding speed (Figs. 11, 12). The angle of inclination of the contours proves that under lubrication conditions (Fig. 12) the sliding speed has a dominant influence on the value of the COF, while under dry friction conditions the influence of these two parameters on the COF is proportional.

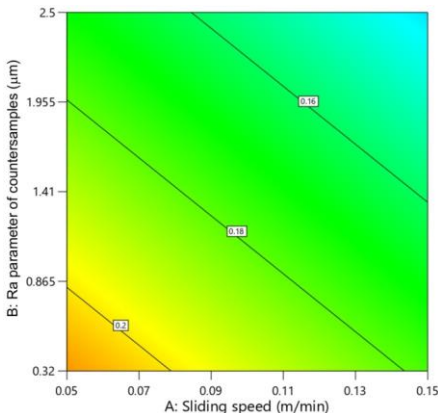


Fig. 11 Contour plot presenting the interaction between sliding speed and Ra parameter of counter samples affecting the COF determined at dry friction conditions

with a sliding speed of 0.05 m/min, the lowest values of the coefficient of friction for both friction conditions were observed for the CuZn30 z4 sheet (Figs. 13, 15). Under the same conditions, the CuZn37 z6 sheet showed the greatest friction. In contrast, the highest coefficients of friction of sheets tested with a sliding speed of 0.15 m/min were observed for the CuZn30 z4 sheet, and the lowest for the CuZn37 z6 sheet (Figs. 14, 15). So, it is clear that the sliding velocity has an important influence on the friction conditions when forming brass sheets.

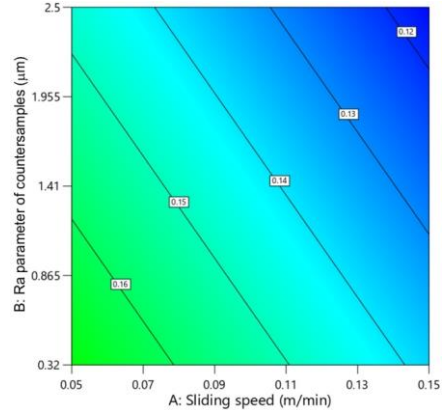


Fig. 12 Contour plot presenting the interaction between sliding speed and Ra parameter of counter samples affecting the COF determined at lubricated conditions

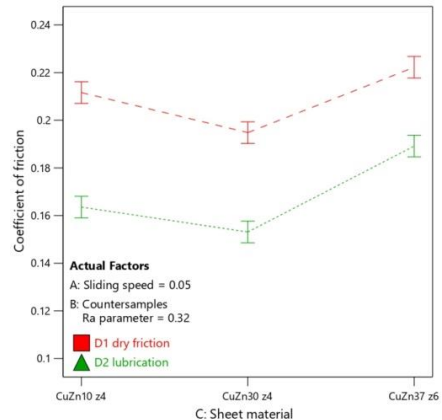


Fig. 13 Interaction plots for the COF determined at a sliding speed = 0.05 m/min and a Ra parameter of the counter samples of 0.32 µm.

The interaction graphs shown in Figs. 13-16 allow a comparison of the dry friction and lubricated conditions. During friction tests

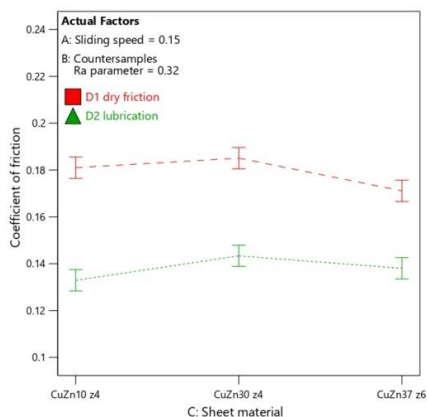


Fig. 14 Interaction plots for the COF determined at a sliding speed = 0.15 m/min and a Ra parameter of the counter samples of 0.32 μm .

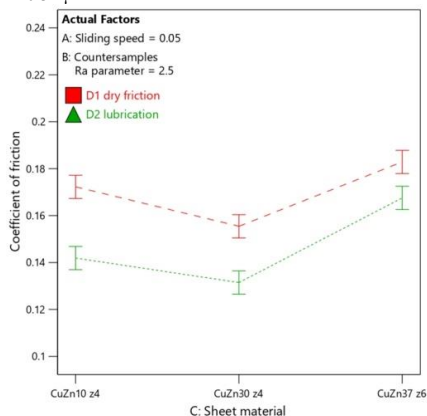


Fig. 15 Interaction plots for the COF determined at a sliding speed = 0.05 m/min and a Ra parameter of the counter samples of 2.5 μm .

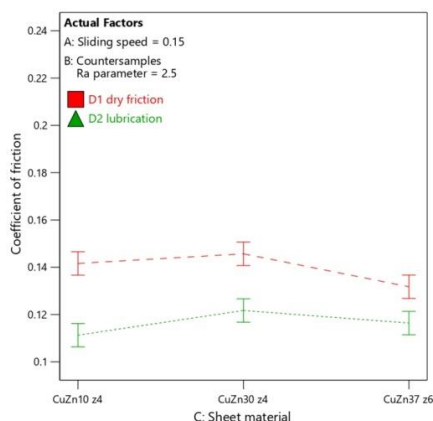


Fig. 16 Interaction plots for the COF determined at a sliding speed = 0.15 m/min and an Ra parameter of the counter samples of 2.5 μm .

CONCLUSIONS

The results of experimental studies to determine the draw bead coefficient of friction of CuZn sheet metals allow the following conclusions to be drawn:

- The coefficient of friction of the sheets decreases with the increase in the average surface roughness of the counter samples, which has been observed for both friction conditions considered.
- As expected, lubrication of the sheet surface resulted in a decrease in the coefficient of friction, however, the effectiveness of lubrication depends on the type of sample material.
- In general, the increase in the sliding speed had the effect of reducing the value of the coefficient of friction.
- A strain hardened material may exhibit stronger metallic adhesive bonding than that the metal characterised by low yield stress and low tendency to strain hardening. Soft metals in contact with a relatively hard tool tend to strongly flattening surface asperities. In this way, the surface of the sheet is susceptible to adhesion and, consequently, the COF increases.
- The most influential input factor found in the experiment range is contact type (F-value 276.55), then the sliding speed (F-value 222.55) and the Ra parameter (F-value 130.74) of the counter samples. The Ra parameter of the counter samples has a proportional impact on the COF for all three materials included in the experiment, while the sliding speed has lower leverage on the changes in the COF of CuZn30 z4.
- Greater lubrication efficiency (lubrication improvement between lubrication and dry friction) has been found for 0.32 μm Ra parameter of the counter samples.

REFERENCES

1. E. Spišák, J. Majerníková, E. Kaščák, P. Mulidrán, V. Rohal, R. Bidulský: *Materials*, 15, 2022, 2299. <https://doi.org/10.3390/ma15062299>.
2. R. Bidulský, M.A. Grande, J. Bidulská, T. Kvačkaj: *Materiáli in Technologije*, 43(6), 2009, 303-307.
3. T. Trzepieciński, J. Slota, E. Kaščák, I. Gajdoš, M. Vojtko: *Materials*, 16, 2023, 2338. <https://doi.org/10.3390/ma16062338>.
4. R. Bidulský, J. Bidulská, T. Kvačkaj, M.A. Grande: *Acta Metallurgica Slovaca*, 29(1), 2023, 34–38. <https://doi.org/10.36547/ams.29.1.1734>.
5. L. Figueiredo, A. Ramalho, M.C. Oliveira, L.F. Menezes: *Wear*, 271(9-10), 2011, 1651-1657. <https://doi.org/10.1016/j.wear.2011.02.020>.
6. T. Trzepieciński, H.G. Lemu: *Metals*, 10, 2020, 47. <https://doi.org/10.3390/met10010047>.
7. P. Mulidrán, E. Spišák, M. Tomáš, J. Majerníková, J. Bidulská, R. Bidulský: *Materials*, 16, 2023, 811. <https://doi.org/10.3390/ma16020811>.
8. A. Losch: In *Sheet Metal Forming Lubricants*; In: Mang, T., Eds.; *Encyclopedia of Lubricants and Lubrication*. Springer: Berlin, Heidelberg, 2014.
9. A. Zajezińska: *Biodegradable Lubricating Greases*. Instytut Nafty i Gazu - Państwowy Instytut Badawczy: Kraków, 2016.
10. S. Plaza, L. Margielewski, G. Celichowski: *Wstęp do tribologii i trochochemia*. Wydawnictwo Uniwersytetu Łódzkiego: Łódź, 2005.

11. R. Bidulský, M.A. Grande, J. Bidulská, M. Vlado, T. Kvačák: High Temperature Materials and Processes, 28, 2009, 175-180.
<https://doi.org/10.1515/HTMP.2009.28.3.175>.
12. A. Schrek, A. Brusilova, P. Sejc, B. Vanko: Acta Metallurgica Slovaca, 27, 2021, 210-213.
<https://doi.org/10.36547/ams.27.4.1254>.
13. J. Varga, T. Tóth, L. Kaščák, E. Spišák: Applied Sciences, 12, 2022, 10638. <https://doi.org/10.3390/app122010638>.
14. T. Trzepieciński: Lubricants, 11, 2023, 28.
<https://doi.org/10.3390/lubricants11010028>.
15. M. Dilmec, M. Arap: International Journal of Advanced Manufacturing Technology, 88, 2016, 747-759.
<https://doi.org/10.1007/s00170-015-8225-5>.
16. S. Dechjarerna, M. Kamonrattanapisu: Applied Mechanics and Materials, 621, 2014, 195-201, 2014.
<https://doi.org/10.4028/www.scientific.net/AMM.621.195>.
17. J. Ma, H. Yang, H. Li, D. Wang, G.J. Li: Transactions of Nonferrous Metals Society of China, 25, 2015, 2924-2931.
[https://doi.org/10.1016/S1003-6326\(15\)63918-8](https://doi.org/10.1016/S1003-6326(15)63918-8).
18. L.A. Carvalho, Z. Lukács: IOP Conference Series: Materials Science and Engineering, 1246, 2022, 012021.
<https://doi.org/10.1088/1757-899X/1246/1/012021>.
19. H.D. Nine: Draw bead forces in sheet metal forming. In *Mechanics of Sheet Metal Forming*, 1st ed.; Koistinen, D.P., Wang, N.M., Eds.; Springer: Boston, USA, 179–211, 1978.
20. D.H. Buckley, W.A. Brainard: In Effect of Strain Hardening on Friction Behaviour of Iron Lubricated with Benzyl Structures. *NASA Technical Note D-661*. National Aeronautics and Space Administration: Washington, D.C., USA, 1974.
21. Z. Wang, T. Suzuki: Procedia Manufacturing, 15, 2018, 474-480. <https://doi.org/10.1016/j.promfg.2018.07.253>.
22. Z.G. Wang, Y. Yoshikawa, T. Suzuki, K. Osakada: CIRP Annals, 63, 2014, 277-280.
<https://doi.org/10.1016/j.cirp.2014.03.050>.
23. W. Czupryk, M. Krawiec: Tribologia, 2, 2008, 127-136.
24. E. Evin, N. Daneshjo, A. Mareš, M. Tomáš, K. Petrovčíková: Applied Sciences, 11, 2021, 2756.
<https://doi.org/10.3390/app11062756>.
25. T. Trzepieciński: Metals, 9, 2019, 988.
<https://doi.org/10.3390/met9090988>.